Discover Materials

RESEARCH Open Access

Examining thermal, structural, and morphological properties of aluminium/TPU composite filaments

Senthilkumar Krishnasamy[1*], G. Swaminathan[1*], Sasikumar Ramachandran[2], V. Parthasarathy[3], Jyotishkumar Parameswaranpillai[4], M. Chandrasekar[5], T. Senthil Muthu Kumar[6] and A. Anto Dilip[1]

*Correspondence:
Senthilkumar Krishnasamy
kmsenthilkumar@gmail.com
G. Swaminathan
swaminathan@psgitech.ac.in
[1]Department of Mechanical Engineering, PSG Institute of Technology and Applied Research, Coimbatore 641062, Tamil Nadu, India
[2]Polymer Engineering Laboratory, Department of Chemistry, PSG Institute of Technology and Applied Research, Coimbatore 641062, Tamil Nadu, India
[3]Department of Physics, Rajalakshmi Institute of Technology, Chennai 600124, Tamil Nadu, India
[4]AU – Sophisticated Testing and Instrumentation Center, Alliance University, Chandapura-Anekal Main Road, Bangalore 562106, Karnataka, India
[5]School of Aeronautical Sciences, Hindustan Institute of Technology & Science, Padur, Chennai 603103, Kelambakkam, Tamil Nadu, India
[6]Department of Mechanical Engineering, Kalasalingam Academy of Research and Education, Krishnankoil 626126, Tamil Nadu, India

Abstract

In this study, thermoplastic polyurethane (TPU)/0.25 wt% of aluminium filler was successfully fabricated using single screw extruder machine. The fabricated filaments were examined for differential scanning calorimetry (DSC), thermogravimetric analysis (TGA), Fourier-transform infrared spectroscopy (FTIR), scanning electron microscopy with energy-dispersive X-ray spectroscopy (SEM-EDS), and X-ray diffraction (XRD). During filament fabrication, the parameters for pure TPU, such as die temperature (160–190 °C), screw speed (400 to 450 rpm), extruder current (2.1 to 2.2 A), were chosen. Similarly, for TPU/aluminium filaments, die temperature (190–160 °C), screw speed (60 rpm), and extruder current (2.9 A) were chosen. Regarding the experimental results, the TGA of TPU/aluminium samples showed higher degradation than pure TPU samples at 850 °C. DSC results showed a minor effect from adding aluminium fillers in the first cycle. However, there was a significant change observed in the melting behavior in the subsequent cycles, which showed enhanced thermal stability and dimensional control at elevated temperatures. FTIR results confirmed interactions between aluminum fillers and TPU, as evidenced by the reduction in the intensity of C=O and N–H stretching bands, which indicated disrupted hydrogen bonds. SEM images showed that aluminium fillers were well embedded in the TPU matrix without any voids, which help in effective load transfer across the matrix. EDS results confirmed the presence of aluminium and oxygen and indicated the formation of Al_2O_3 during filament extrusion. Besides, XRD results exhibited a sharp crystalline peak and indicated improved structural stability due to adding aluminium fillers into TPU matrix.

Highlights

- Aluminium and TPU samples were fabricated using a single screw extruder.
- TGA results exhibited a final residue of aluminium/TPU of 5.60% at 850 °C.
- SEM revealed rougher surfaces and enhanced interactions.
- XRD analysis exhibited sharp crystalline peaks, confirming the presence of aluminum in TPU matrix.

Keywords Thermoplastic polyurethane, Aluminium filler, Single screw extruder, Thermal stability

1 Introduction

Thermoplastic polyurethane (TPU) has attracted significant attention among the polymers used in additive manufacturing techniques due to its greater elasticity, flexibility, good adhesion, resistance to corrosion, and toughness [1]. These properties are highly preferred in various applications, such as footwear, automotive components, agriculture, film and sheet, seal and gasket, textile coating, sports and leisure, and flexible electronics [2]. The TPU market is projected to grow from $3.01 billion (USD) in 2023 to $4.71 billion (USD) by 2030, exhibiting a compound annual growth rate (CAGR) of approximately 6.89% during the forecast period [3].

Princi [4] reported that TPU could be described to bridge the gap between rubber and plastics; thus, the TPU imparts elasticity and high abrasion resistance to the materials. Therefore, it is highly suitable for biomedical applications. Further, TPU's properties can be altered by incorporating various fillers such as metal-based, carbon-based, ceramic-based, etc., to improve mechanical, thermal, and electrical properties [5]. In this experimental study, aluminium fillers were incorporated into TPU matrices, and their various properties were examined to analyse their suitability for lightweight and temperature-based applications (e.g., automotive, and aerospace). Because the TPU has good thermal stability, and its degradation temperature commences at ~ 230 °C to 300 °C [2].

Aluminium fillers can be reinforced with thermoplastic polymers as powder, nanoparticles, or flakes based on the desired properties [6]. Additionally, the major properties of aluminium fillers include (i) higher thermal conductivity (~ 204 W/m·K) [7, 8], (ii) lightweight [9] (iii) higher electrical conductivity (~ 37.7 MS/m) [10, 11], and (iv) corrosion resistance [12]. Thus, incorporating the aluminium fillers into the TPU matrix enhances properties, such as mechanical strength, thermal performance, electrical conductivity, dimensional stability, and barrier properties. For example, surface-modified alumina/TPU samples exhibited an 80.6% improvement in thermal conductivity due to the addition of 40% 3-Aminopropyltriethoxysilane (APTES)-treated alumina fillers [13].

Thus, many researchers have explored the use of various fillers by incorporating them into polymers, studying their properties, and adapting them for different applications. Bapan et al. [14] fabricated Cloisite 30B/polyurethane (PU) and Claytone acetylacetone-modified polyamine (APA)/PU nanocomposites using a twin-screw extruder at 190 °C under a nitrogen atmosphere. The clay loading varied from 1wt.% to 5wt.%, and the samples were subsequently shaped into films using a compression moulding machine. The results reported that filler-reinforced samples exhibited improved thermal stability compared to pure PU samples. For example, the degradation temperature at 5% weight loss increased from 317 °C for neat PU to 329 °C when reinforced with 5wt.% Claytone APA. This improvement was attributed to the enhanced dispersion of the clay fillers in the PU matrix and their ability to restrict the mobility of polymer chain. In another study [15], laponite/TPU nanocomposites were fabricated by varying the laponite fillers from 0.5wt.% to 10wt.% and were analysed using dynamic mechanical analysis (DMA) and XRD. DMA results showed that laponite fillers improved the stiffness of nanocomposites, with the highest increase observed at 10 wt.%, and enhanced damping properties at 5 wt.% and 10 wt.%. Besides, all samples exhibited a rubbery plateau at temperatures above − 46.3 °C (corresponds to T_g). XRD analysis revealed that agglomeration of clay platelets at 5wt.% and 10wt.% reduced the dispersion effectiveness. Furthermore, the degree of crystallinity of the TPU matrix increased with higher laponite filler loading.

In another study [16], h-BN and TPU matrix samples were fabricated using fused filament fabrication techniques and examined various characterization techniques. The researchers observed DSC results that the TPU matrix was suitable for fabricating 3 Dprinted composite samples. Besides, they found that incorporating h-BN fillers within the TPU matrix did not influence the printing quality. Jingshui Xu et al. [17] observed an improved thermal behaivor of 4,4'-Methylenediphenyl Diisocyanate-Modified Montmorillonite (MDI-MMT)/TPU composite samples than pure TPU. This improvement was reported by TGA whereby the char residue value of TPU was increased from 3.47% to 5.62% for MDI-MMT/TPU nanocomposites. Bashpa et al. [18] examined XRD and thermal stability of TPU matrix reinforced with multi-walled carbon nanotubes. They observed that the crystallinity was found to be doubled in composite samples than pure matrix. The thermal stability of 3% of filler reinforced composites showed considerable enhancement from the TGA results.

Based on the literature review, higher filler loading was used to produce composite samples. In contrast to higher filler loading, in this study 0.25wt.% of aluminium fillers were incorporated into the TPU matrix and proposed various characterization techniques. Thus, it could be a cost-effective and scalable way of producing composite samples and most importantly filler agglomeration can be reduced.

Our work examined (DSC, TGA, XRD, FTIR, and SEM) extruded filaments of TPU and TPU–Al samples, rather than bulk polymer samples, coatings, or films. The fabricated filaments are intended for use in 3D printing (FDM) for high-temperature applications in automotive and aerospace sectors. For example, DSC results revealed that aluminium fillers improved thermal and dimensional stability at elevated temperatures, making the samples produced suitable for repeated heating and cooling cycles. Furthermore, the addition of only 0.25 wt.% aluminium filler enhanced crystalline order and interfacial bonding in the filaments, which is particularly beneficial for additive manufacturing applications.

2 Experimental details

2.1 Materials

The materials, such as thermoplastic polyurethane (TPU) pellets and aluminum fillers, were purchased from SRL Chemicals, Coimbatore, India, for the preparation of filaments. Figure 1 (a-b) shows the pure TPU pellets and aluminum fillers. The major properties of TPU and aluminum fillers are given in Tables 1 and 2.

2.2 Methods

2.2.1 Preparation of TPU and TPU/Aluminium composite filaments

The single-screw extruder, consisting of a screw, barrel, hopper, head, gearbox, and die, was used to make thermoplastic polymer filaments, as shown in Fig. 2. Typically, the gearbox system consists of a motor, reducer, and coupling or V-belt drive. The primary function of the gearbox system is to rotate the screw within a predetermined speed range. It ensures that the screw turns steady and uniform rotation under a specific torque. This helps in completing plastic melting as well as plasticization and allowing the material to push out of the barrel based on the requirement.

A specific temperature (refer to Table 3) was applied to the plastic in the barrel when the single-screw extruder began the extrusion production to promote the plasticization

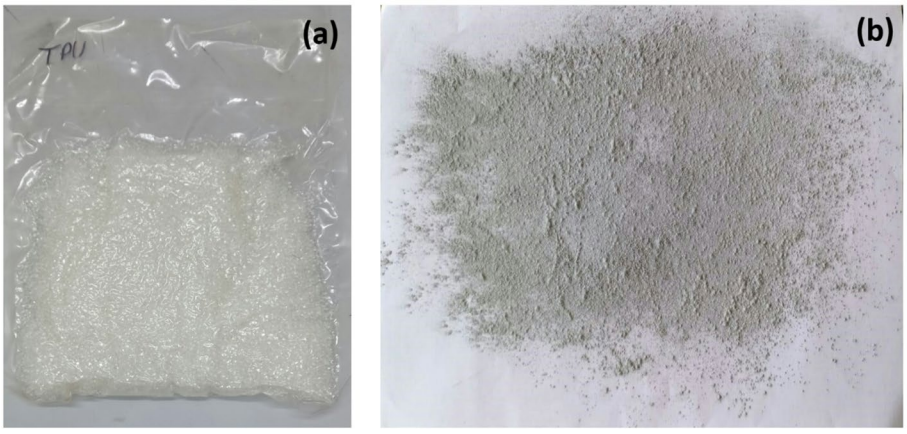

Fig. 1 Materials used (**a**) thermoplastic polyurethane (TPU) pellets and (**b**) aluminium filler

Table 1 Major properties of TPU [19]

Material	Tensile strength (MPa)	Young's modulus (MPa)	Elongation at break (%)	Glass transition temperature (°C)	Melting point (°C)
TPU	25–50	10–100	500	−50 to −30	> 150

Table 2 Major properties of aluminium filler [7, 20]

Type of material	Density (g/cm^3)	Thermal conductivity (W/m/K)	Coefficient of thermal expansion $\times 10^{-6}$/°C
Aluminium filler	2.7	204	26.7 (20 to 400 °C)

of the plastic under the action of the screw. The barrel cooling system was used to control the temperature rise inside the barrel caused by extrusion and friction, ensuring a smooth extrusion output. The screw mechanism forced the material through the die, where it was shaped by the die, post-extrusion shaping, or both. The product was then set into shape by cooling while maintaining its structural integrity. The apparatus used for this process is called the post-extrusion apparatus, and the entire system is referred to as the extrusion line. Under the pressure created during extrusion, the plastic raw material, in the form of pellets, was melted into a uniform, consistent melt through the extrusion system. The material was continuously forced through the screw and die to form a filament.

The temperature and pressure of the four-barrel heating zones were controlled by a digital controller, as shown in Fig. 2 (b-c). The filament thickness was controlled by adjusting the engine speed (rpm) and applied current (A) of the extruder. The four heating zone temperatures were set (refer to Table 3), and once the desired temperature was reached, the TPU pellets were transferred into the hopper. The engine rpm was then gradually increased without exceeding the required ampere limit. During the extrusion process, the filament thickness was adjusted to a range of 1.7 mm to 1.8 mm in diameter by varying the rpm and amperage of the extruder, ensuring suitability for 3D printing applications.

The heating zone temperatures were further modified (refer to Table 3) for the TPU-aluminum filler composite filament, as the same temperature settings as TPU were

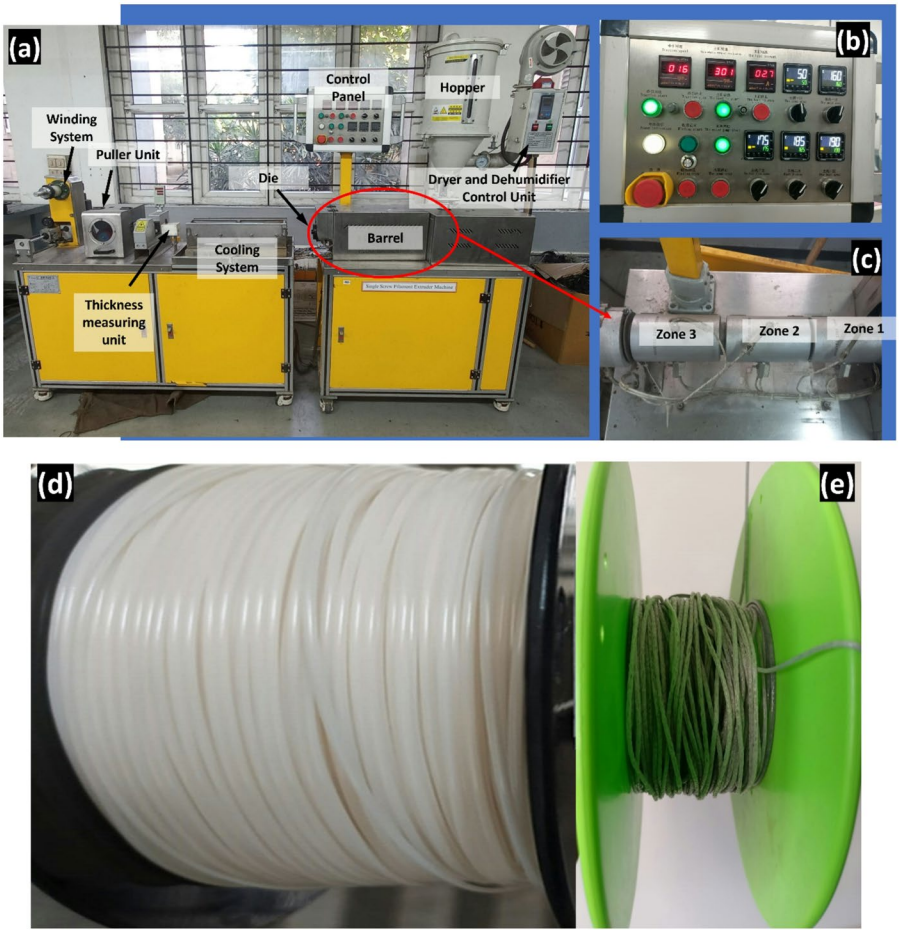

Fig. 2 Single screw extruder machine for fabricating TPU and aluminium/TPU samples: (**a**) full view of the machine set up, (**b**) control panel displays temperature and screw speed settings, (**c**) heating zones (zones 1, 2, 3 and 4), (**d**) pure TPU filament, and (**e**) aluminium/TPU composite filament

Table 3 Major parameters used to fabricate the pure TPU and aluminium/TPU filaments

Parameters	TPU filament	Aluminium/TPU filament
Zone 1 temperature (°C)	160	190
Zone 2 temperature (°C)	170	180
Zone 3 temperature (°C)	180	170
Zone 4 temperature (°C)	190	160
Die temperature (°C)	190	160
Screw speed (rpm)	400–450	60
Extruder current (A)	2.1–2.2	2.9
Filament diameter (mm)	1.7–1.8	1.7–1.8

unsuitable. This difference was likely due to thermal interactions between aluminum powder and TPU, requiring adjustments in processing parameters. Furthermore, the pure TPU and TPU-aluminum composite filaments were subjected to structural, thermal, and morphological characterization. Table 3 presents the major processing parameters, including temperature, rpm, and current, used to fabricate the pure TPU and TPU-aluminum composite filaments using a single-screw extruder.

2.3 Characterization

2.3.1 Thermogravimetric analysis (TGA)

TGA measurements of pure TPU and TPU + aluminium filaments were performed using a Perkin Elmer TGA 4000 instrument at a heating rate of 20 °C min^{-1}. Small portions of the filaments, weighing 5 mg, were placed in a ceramic crucible, and the measurements were carried out under a nitrogen atmosphere at a flow rate of 30 mL min^{-1}. The temperature of the test was between 50 °C and 850 °C.

2.3.2 Differential scanning calorimetric (DSC)

DSC test was conducted using a Perkin Elmer DSC 6000 instrument to examine the thermal behavior of TPU and TPU + aluminium samples. Approximately 5 mg was measured and placed in an aluminium pan along with an empty aluminum pan was used as a reference. Each sample was heated from − 50 °C to 250 °C by maintaining a heating rate of 10 °C min^{-1} under a nitrogen atmosphere with a flow rate of 20 mL min^{-1} to prevent oxidation.

2.3.3 Fourier transform infrared spectroscopy (FTIR)

Fourier Transform Infrared (FTIR) spectra of TPU and TPU + aluminium filaments of ~ 10 mg were recorded using a Shimadzu IR Spirit-X. The FTIR spectra were ranged from 4000 cm^{-1} to 500 cm^{-1}.

2.3.4 Scanning electron microscopy (SEM) with energy dispersive X-ray spectroscopy (SEM-EDS)

In this study, a JCM-7000 benchmark SEM (JEOL) was used to get scanning electron microscope images of aluminium filler powders. Then, the interaction between TPU, aluminium fillers and EDS spectra were analysed using Zeiss scanning electron microscopy (SIGMA, Carl Zeiss, Germany). For the SEM and EDS tests, an approximately 5 mm length filament was used.

2.3.5 X-Ray diffraction analysis

The structural characterization was performed using an Anton Paar XRDynamic 500 diffractometer with Cu-Kα radiation (λ = 1.5406 Å). During the test, the samples were scanned in the 2θ range (from 10° to 90°) and the scanning rate of 0.02°/sec was maintained.

3 Results and discussion

3.1 Thermogravimetric analysis (TGA)

Figure 3 illustrates the TGA results of pure TPU and Al-filled TPU filaments. Both filament samples start to degrade at ~ 300 °C, showing the onset of significant weight loss. This observation suggests that the thermal decomposition of TPU samples was primarily due to the breakdown of urethane linkages [21]. Since both filaments had the same onset temperature, this indicates that the addition of 0.25% aluminum did not alter the thermal initiation process of TPU samples.

Furthermore, Fig. 3 reveals that a sharp weight loss was observed between 300 °C and 500 °C in both filaments, corresponding to the main decomposition phase. This phase was attributed to the thermal breakdown of the soft and hard segments of TPU

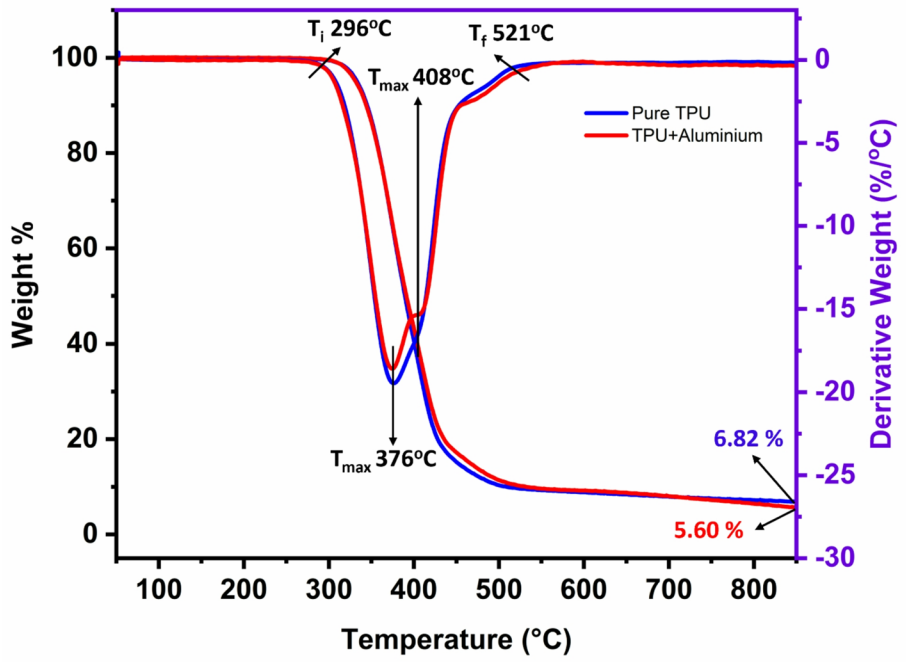

Fig. 3 TGA thermogram of pure TPU and TPU/aluminium filament samples

polymers, where the soft segments (i.e., polyol-based) decomposed first, followed by the hard segments (urethane groups and possibly aromatic components) [22]. It is also observed that the rate of decomposition is 0.8 wt.% per °C for both samples, which indicate the addition of aluminium-filler does not affect the decomposition behavior. Regarding weight loss, both pure TPU and the aluminium-filled TPU exhibit a two-stage degradation. The maximum degradation temperature was observed to be similar during the first and second stage degradation for both samples and it was found to be 376 °C and 408 °C, respectively.

Further, both the pure TPU and aluminium-filled TPU exhibit similar char-yield up to 700 °C. Beyond this temperature, the aluminium-filled TPU (5.6 wt%) have undergone slightly more degradation than the pure TPU (6.82 wt%). This slight shift suggests the influence of aluminum on the decomposition kinetics [23]. Based on these observations, 0.25% aluminum had only a minor effect on thermal stability.

3.2 Differential scanning calorimetry (DSC)

Figure 4a shows the DSC plots of the pure TPU and 0.25% aluminum-filled samples. The results revealed notable differences in the thermal responses of these samples. The first heating cycle of the DSC thermogram shows a small endothermic peak (between 147 °C and 192 °C) with T_{max} at about 177 °C, which infers the pure TPU started to melt at this temperature that could be due to the low molecular weight of TPU and/or the part of its soft segment, following a significant endothermic peak was observed at 203 °C indicates the melting of TPU containing hard and soft segments. Subsequent cooling thermogram exhibits an exothermic peak at 88 °C indicates the crystallization of TPU. A similar trend was observed in the aluminum-filled samples that is the melting peaks exhibited at 187 °C and 203 °C and the exothermic peak was observed at 88 °C during cooling reveals there were no significant changes due to the addition of aluminium into

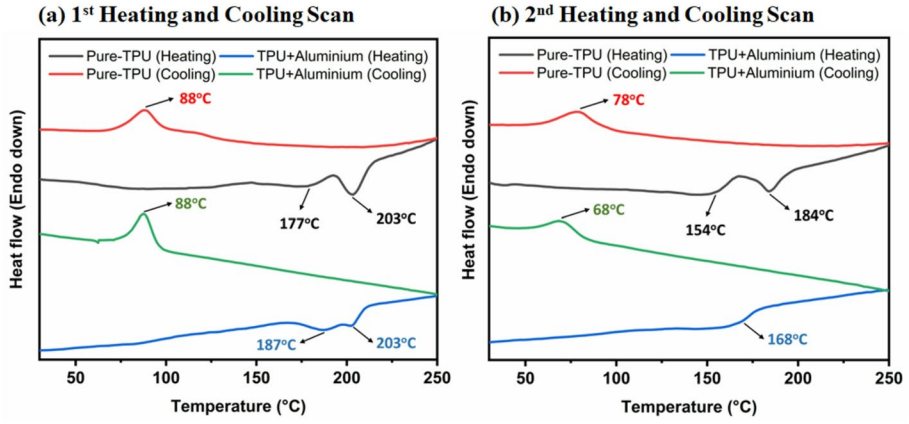

Fig. 4 DSC thermogram of pure TPU and TPU/aluminium filament samples

the TPU. However, the second heating and cooling cycles of the TPU and aluminium-filled TPU exhibit considerable changes by decreasing their melting and crystallization temperatures, as shown in Fig. 4b. This could be due to the degradation of the samples to about 250 °C during the previous heating cycle. This resulted in reduction in molecular weight of the TPU as compared to the original sample. Moreover, the second heating cycle of the aluminium-filled TPU exhibits lower melting temperature at about 168 °C compared to that of pure TPU (T_m: 154 °C and 184 °C) that may be due to the homogeneous distribution of aluminium that contributes to the reduction of melting temperature of TPU. The single melting peak in the composites may be due to the enhanced crystalline order in the presence of aluminium. The consistent reduction in melting temperature of the aluminum-filled samples was attributed to the aluminum fillers influencing both the thermal energy absorption and dissipation dynamics of the TPU matrix filament samples possibly due to the filler-polymer and filler-filler interaction. Jing et al. [24] examined the nucleation/barrier effects of graphene oxide fillers in TPU samples. They reported that the onset crystallization temperature increased with the addition of fillers. Furthermore, the exotherms were wider and shallower, resulting in faster nucleation while crystal growth was restricted.

When temperature exceeded 150 °C, both pure TPU and aluminum-filled TPU samples exhibited an endothermic peak (between 150 °C and 250 °C), ascribed to the melting of crystalline regions as well as thermal softening of hard segments in the TPU matrices. Similar behavior was observed in an earlier report [25], whereby crystalline and thus the thermal transitions of TPU-reinforced samples are influenced by fillers (TiO_2 and multi-walled carbon nanotubes). In another work, Barick and Tripathy [26] examined the DSC behavior of filler–matrix interaction. They observed that the soft segment melting and crystallinity of organically modified layered silicate/TPU samples increased. This observation was attributed to nucleation and restriction in chain mobility.

The aluminum-filled sample showed a less intense endothermic peak compared to the pure TPU samples (Fig. 4a). However, this peak was shifted to a higher temperature compared to pure TPU. This behavior was attributed to the aluminum particles disrupting the crystalline structure and altering the softening transitions in the hard segments. Such broadening of thermal transitions of TPU composites reinforced with boron nitride and liquid metal were reported in reference [27]. This disruption could improve

thermal resistance and reduce deformation at higher temperatures, which is beneficial for applications requiring dimensional stability under thermal stress.

Furthermore, the aluminum-filled samples showed lower melting temperature in the second heating cycle, as shown in Fig. 4b, indicating that aluminum acted as a thermal conductor. This increased thermal conductivity can enhance heat transfer within the TPU matrices, reducing the melting temperature of TPU. This thermal conductivity property of aluminum was further supported by the residue values from the TGA results (Fig. 3), showing 5.60% residue for aluminum-filled TPU samples compared to 6.82% for pure TPU samples.

3.3 FTIR

Figure 5 illustrates the FTIR observations of pure TPU and aluminium/TPU samples. It shows structural and interactional changes from the TPU matrix due to the incorporation of aluminium fillers. For instance, the TPU and aluminium/TPU samples exhibited a strong C = O stretching (1725–1740 cm^{-1}). This observation was attributed to the carbonyl groups in the urethane linkages of TPU matrices. Though, the aluminium/TPU samples exhibited lesser intensity than the pure TPU samples [28]. This observation was attributed to the interaction of aluminium fillers and TPU matrix; which could be disrupted the inter-chain hydrogen bonds. This led to a weaker interaction with the carbonyl groups. Besides, the aluminium/TPU samples exhibited N-H stretching (~ 3300–3500 cm^{-1}); this was lesser intense in these samples. Similarly, the aluminium/TPU samples showed C-N stretching (~ 1530 cm^{-1}) with a lesser intensity. All these could support that the aluminium fillers were disrupted the inter-chain hydrogen bonds in TPU. Further, the C-O and -(C = O)-O- stretching were observed between 1000 and

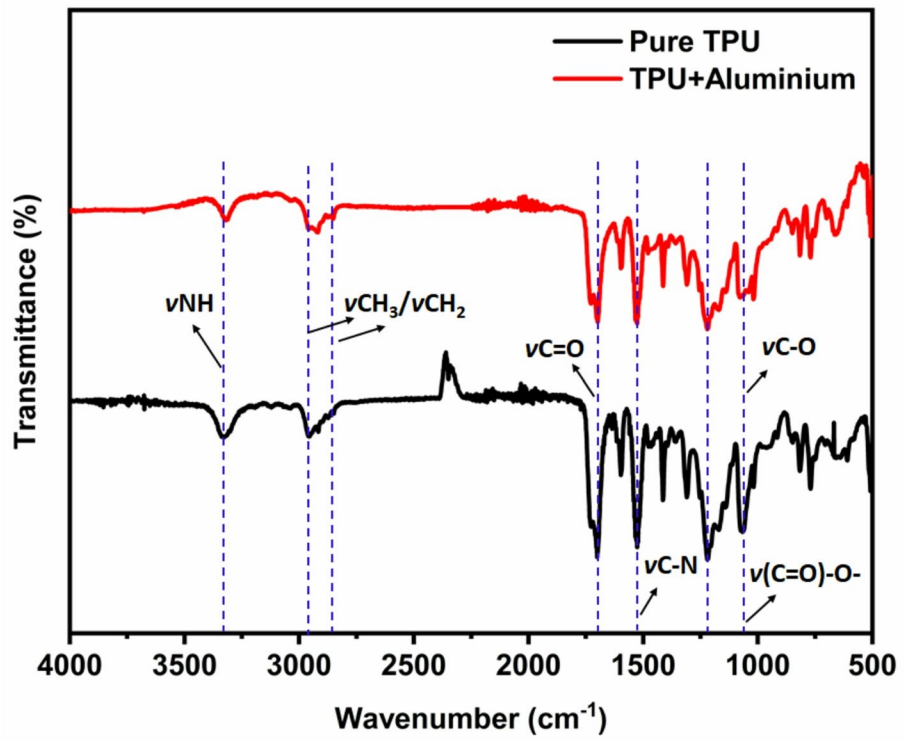

Fig. 5 FTIR graph of pure TPU and TPU/aluminium filament samples

1300 cm^{-1}; and the aluminium samples exhibited a slight change in intensity. This was ascribed to the interaction between the aluminium fillers and TPU hard segments; thus, affecting structural dynamics [29].

Thus, Fig. 5 shows that the aluminium/TPU samples exhibited reduction in the intensity of hydrogen bonds. This could be the indication of improved interactions between aluminium and TPU matrix. The same observation was further supported by the TGA results (Fig. 3). Whereby the improved thermal stability was observed by the aluminium/TPU samples. Because the aluminium fillers could disrupt the crystalline structures; this could help in enhancing the heat dissipation behavior. Table 4 shows the major observations of FTIR peaks which were observed in Fig. 5.

3.4 Scanning electron microscopy (SEM)

The SEM images were taken and analyzed to illustrate the morphological characteristics of aluminum powder, pure TPU, and TPU reinforced with aluminum fillers. Figure 6(a) shows the distinct morphology of aluminum powder, indicating an irregularly shaped structure with varying particle sizes ranging from 25 to 68 µm. The EDS spectrum in Fig. 6(b) confirms the presence of aluminum as the primary element, ensuring the purity of the fillers incorporated into the TPU matrix. It is also observed that a significant amount (~3.5%) of oxygen is present in the powder due to oxidation of Al to Al_2O_3 in the presence of air.

Figures 7(a) and 7(b) depict the microstructural features of an extruded filament made of pure TPU at 150× and 2500× magnifications, respectively. The TPU filament surface appears relatively smooth and homogeneous, lacking any visible porosity or significant defects. This observation suggests a well-formed polymer structure with minimal internal voids. Also, the parameters used to extrude the filament are optimized. However, the addition of aluminum fillers significantly alters the TPU morphology, as evident from Figs. 8(a) and 8(b). The TPU/aluminum composite filament exhibits a rougher texture and well-dispersed aluminum particles, confirming successful filler integration. At 2500× magnification (Fig. 8(b)), aluminum fillers appear embedded within the TPU matrix, demonstrating a good interfacial interaction between the polymer and filler. Such interactions are essential for effective load transfer and mechanical reinforcement.

The presence of aluminum within the TPU matrix suggests that filler incorporation enhances structural integrity by reducing polymer chain mobility and increasing dimensional stability. This is particularly beneficial for applications requiring enhanced mechanical performance, such as aerospace and automotive industries. Furthermore, the well-dispersed nature of aluminum fillers indicates that the fabrication method

Table 4 Major observations of FTIR peaks

Wave number	Details of functional group	Major observations
3300 cm^{-1} to 3500 cm^{-1}	N-H stretching	The disruption of inter chain hydrogen bonds was observed.
1725 cm^{-1} to 1740 cm^{-1}	C = O stretching (carbonyl)	It was observed that the interaction of Aluminium/TPU reduced the H-bond
2964 cm^{-1} to 2852 cm^{-1}	CH_3 and CH_2 stretching	The presence of aliphatic groups in TPU was observed
1530 cm^{-1}	C-N stretching	The stretching of C-N in urethane group was observed
1000 cm^{-1} to 1300 cm^{-1}	C-O and -(C = O)-O- stretching	The stretching vibrations of hydrogen bonded ester in urethane group was observed

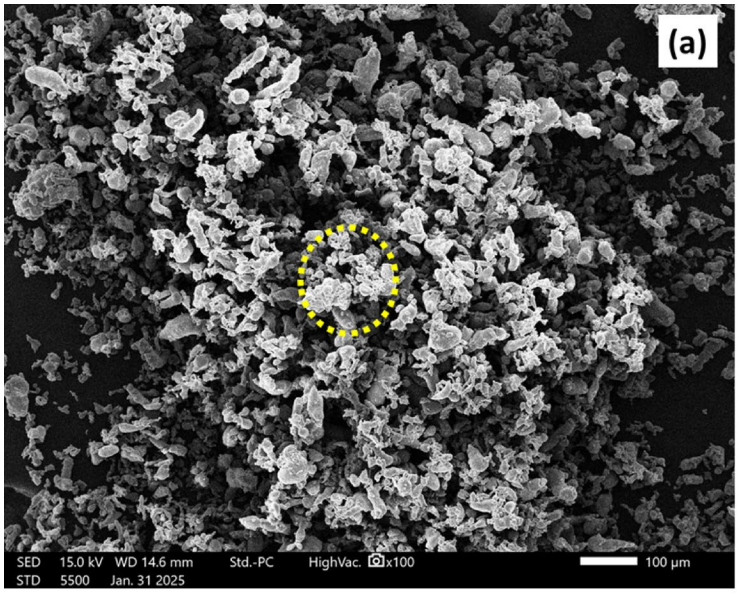

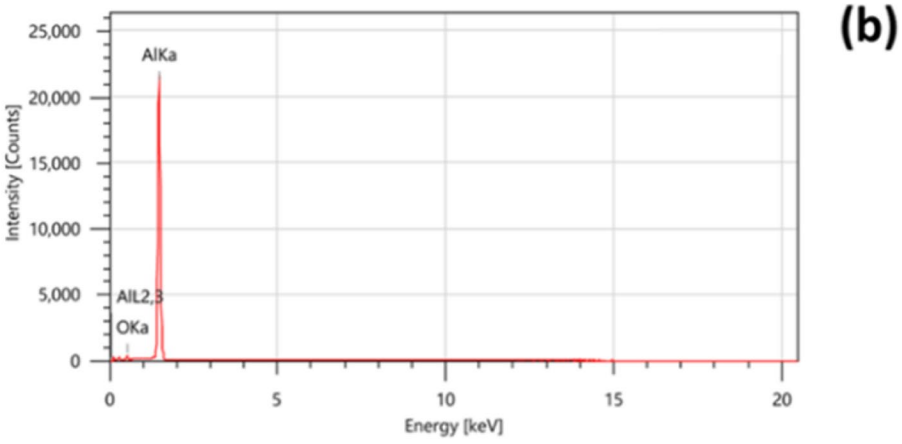

Name	O	Al	Total
Spc_001	3.42	96.58	100.00
Average	3.42	96.58	
Standard Deviation			

Fig. 6 **(a)** SEM image of aluminium powder showing irregular morphology (average particle size 46.2 ± 11.7 µm, range 25–68 µm) and (**b**) corresponding EDS spectrum confirming elemental composition

employed, using a single-screw extruder, facilitated uniform dispersion of the filler, which ensures the improved properties of the composite materials.

From Fig. 8, it can be observed that the aluminium fillers are observed to be well embedded within the TPU matrix without voids, confirming strong adhesion between the filler and polymer. This good interfacial interaction is attributed to two mechanisms, which are the disruption of inter-chain hydrogen bonds in TPU as evidenced by FTIR (Fig. 5) that facilitates closer filler–matrix contact and uniform dispersion of aluminium fillers achieved through extrusion, which promotes effective load transfer across the matrix. Such bonding improves stress transfer efficiency and enhances the mechanical stability of the composite.

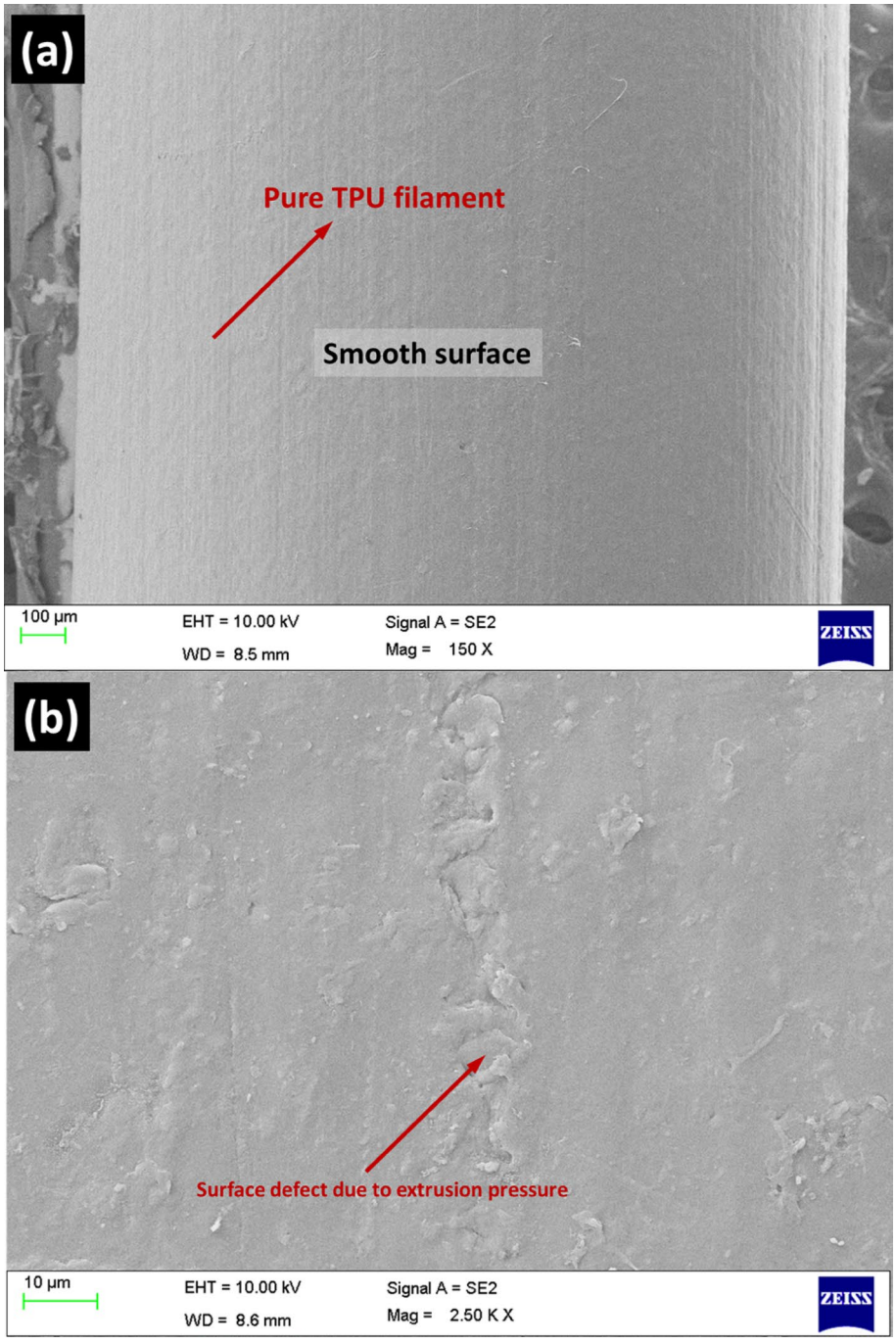

Fig. 7 SEM images of pure TPU at (**a**) 150X and (**b**) 2500X magnifications showing the smooth and relatively lesser defected surfaces

3.5 X-Ray diffraction analysis

Figure 9 shows the X-ray diffraction patterns of the filaments made of pure TPU and TPU/aluminum composites. The XRD diffractogram reveals that pure TPU exhibits broad peaks due to the presence of amorphous regions in the polymeric structure. This is consistent with previous studies [30, 31] and indicating that TPU lacks significant crystalline domains due to its flexible polymer chains. The incorporation of aluminum fillers results in the appearance of sharp peaks corresponding to the crystalline nature

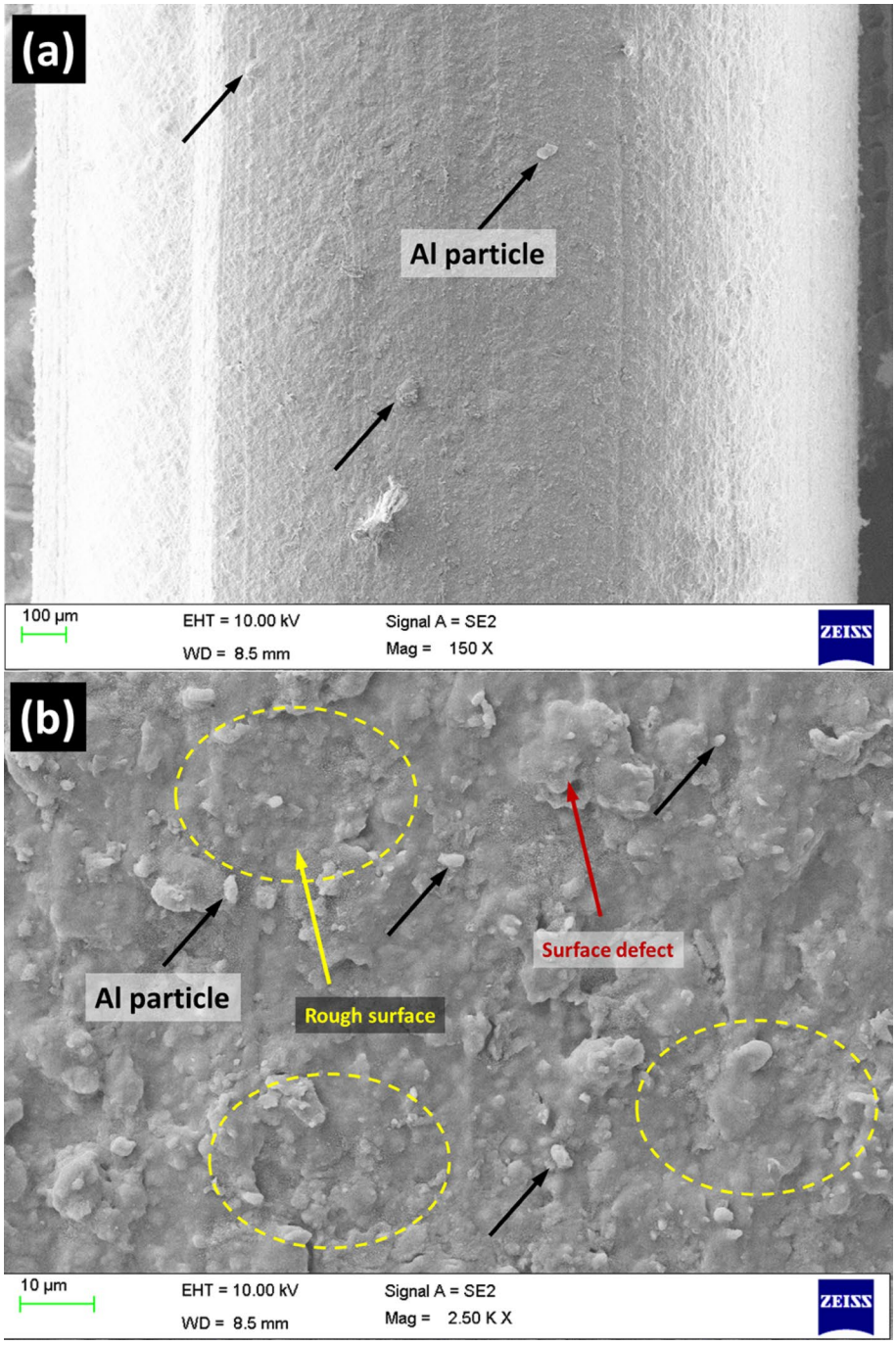

Fig. 8 SEM images of TPU with Al filler addition at (**a**) 150X and (**b**) 2500X magnifications showing the adhesion of Al powder particle and relatively rough surface

of aluminum. These peaks show that the presence of uniformly distributed metallic particles within the TPU matrix. Moreover, the slight shift in peak positions show that certain degree of polymer-filler interaction is occurred that potentially altered the TPU molecular arrangement.

The higher degree of crystallinity observed in TPU/aluminum composites is expected to contribute to the observed improved hardness, stiffness, and resistance to thermal degradation. These findings are in line with the previous findings that showed improved

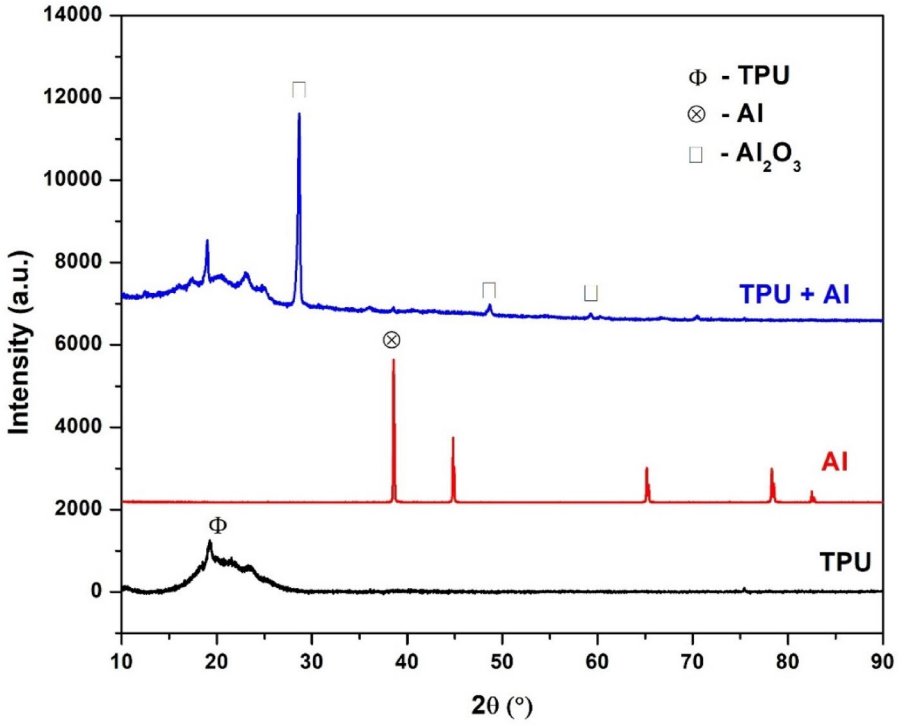

Fig. 9 X-ray diffractogram of TPU and TPU + Al composite

structural stability in TPU composites reinforced with metallic/ceramic fillers [32, 33]. In addition to the crystalline peaks of Al, distinct reflections corresponding to Al_2O_3 were observed indicating that the partial oxidation of aluminium particles occurred during extrusion process. These peaks confirm the coexistence of metallic aluminium and its oxide in the TPU matrix. The clearer diffractogram (Fig. 9) with labelled peaks provides direct evidence of both phases.

4 Conclusions

In this study, the incorporation of aluminium fillers into the TPU matrix showed their possible potential to improve thermal and structural properties. The fabrication was performed using a single screw extruder, which enabled a uniform dispersion of aluminium fillers, ensured better interfacial bonding, and produced high-quality filaments. The major results and observations of the experimental work are described below:

- TGA results reported that the onset degradation temperature for pure TPU and aluminium-filled samples was observed to be ~300 °C. Major weight loss was observed between 300 °C and 500 °C. Regarding char yield, the aluminium-filled samples exhibited 5.6 wt.% compared to the pure TPU samples (6.82 wt.%).
- DSC results of extruded filaments were cycle dependent. The first cycle did not show any significant differences between the pure TPU and aluminium-filled samples. During the second cycle, the aluminium-filled samples showed a lower melting temperature. This indicates that the aluminium filler acted as a thermal conductor. This increased thermal conductivity can enhance heat transfer within the TPU matrix, reducing the melting temperature of TPU polymer.
- FTIR results showed the disruption of hydrogen bonds.

- SEM images of pure TPU samples showed smooth and homogeneous surfaces, which indicate a well-formed TPU structure with minimal internal voids. The aluminium-filled samples, on the other hand, showed a rougher texture and well-dispersed aluminium particles. This indicates that the samples had good interfacial bonding between the matrix and fillers. This could support improved load transfer in structural applications.
- Furthermore, XRD analysis confirmed the presence of aluminium fillers, which contributed to increased structural order and improved stability of the composites. Despite the relatively low filler content (0.25 wt%), the results suggest that increasing the filler loading may further improve thermal resistance and mechanical strength.

For future work, optimization of aluminium fillers and processing conditions is recommended to further improve performance of composite. Additional experimental studies could explore the suitability of using aluminium/TPU composites for advanced applications such as aerospace and automotive and improved thermal conductivity.

Author contributions
Senthilkumar Krishnasamy: Conceptualization, Experiment, Draft writing and editing the manuscript. G. Swaminathan: Characterization, Analysis, Supervision and editing the manuscript. Sasikumar Ramachandran: Fabrication, Testing and editing the manuscript. V. Parthasarathy: Editing and reviewing. Jyotishkumar Parameswaranpillai: Testing, analysis and editing the manuscript. M. Chandrasekar: Validation and editing the manuscript. T. Senthil Muthu Kumar: Resources and editing the manuscript. A. Anto Dilip: Fabrication and sample preparation

Funding
This research did not receive any specific grant from funding agencies in the public, commercial, or not-for-profit sectors.

Data availability
The raw and processed data required to reproduce the results will be shared upon request.

Declarations

Ethics approval
Not applicable.

Competing interests
Senthilkumar Krishnasamy and T. Senthil Muthu Kumar are Editorial Board Members of Discover Materials. They were not involved in the handling, peer review, or decision-making process for this manuscript. The other authors declare no competing interests.

Received: 3 July 2025 / Accepted: 26 December 2025
Published online: 22 January 2026

References

1. Backes EH, Harb SV, Pinto LA, de Moura NK, de Melo Morgado GF, Marini J, et al. Thermoplastic polyurethanes: synthesis, fabrication techniques, blends, composites, and applications. J Mater Sci. 2024;59:1123–52.
2. Allami T, Alamiery A, Nassir MH, Kadhum AH. Investigating physio-thermo-mechanical properties of polyurethane and thermoplastics nanocomposite in various applications. Polym Basel. 2021;13:2467.
3. Thermoplastic, Polyurethane. (TPU) Market Insights 2025.
4. Princi E. Rubber: science and technology. Walter de Gruyter GmbH & Co KG; 2019.
5. Mokoena TE, Magagula SI, Mochane MJ, Mokhena TC. Mechanical properties, thermal conductivity, and modeling of Boron nitride-based polymer composites: a review. Express Polym Lett. 2021;15:1148–73.
6. Yang S, Li W, Bai S, Wang Q. Fabrication of morphologically controlled composites with high thermal conductivity and dielectric performance from aluminum nanoflake and recycled plastic package. ACS Appl Mater Interfaces. 2018;11:3388–99.
7. Nurul Hidayah I. Properties of single and hybrid aluminum and silver fillers filled high-density polyethylene composites. J Thermoplast Compos Mater. 2012;25:209–21.
8. Kumar M, Upadhyay S, Bansal L, Verma R. An experimental and analytical investigation to determine thermal conductivity of epoxy-filler composites for space applications. Cryogenics. 2024;144:103973.
9. Kayode O, Akinlabi ET. An overview on joining of aluminium and magnesium alloys using friction stir welding (FSW) for automotive lightweight applications. Mater Res Express. 2019;6:112005.
10. Desai PD, James HM, Ho CY. Electrical resistivity of aluminum and manganese. J Phys Chem Ref Data. 1984;13:1131–72.

11. Ryvkina NG, Nezhnyi PA, Kudinova OI, Chmutin IA, Grinev VG, Novokshonova LA. Electrical and heat conduction properties of polymerization-filled composites based on ultra-high-molecular-weight polyethylene and nano-and micron-sized aluminum particles. Russ J Phys Chem B. 2019;13:831–7.
12. Gnedenkov SV, Sinebryukhov SL, Egorkin VS, Vyalyi IE, Mashtalyar DV, Nadaraia KV, et al. Formation and properties of composite coatings on aluminum alloys. Russ J Inorg Chem. 2017;62:1–11.
13. Wondu E, Lule Z, Kim J. Thermal conductivity and mechanical properties of thermoplastic polyurethane-/silane-modified Al2O3 composite fabricated via melt compounding. Polymers. 2019;11:1103.
14. Adak B, Butola BS, Joshi M. Effect of organoclay-type and clay-polyurethane interaction chemistry for tuning the morphology, gas barrier and mechanical properties of clay/polyurethane nanocomposites. Appl Clay Sci. 2018;161:343–53.
15. Arenas JP, Castaño JL, Troncoso L, Auad ML. Thermoplastic polyurethane/laponite nanocomposite for reducing impact sound in a floating floor. Appl Acoust. 2019;155:401–6.
16. Luo M, Yang T, Wang T, Yan Z, Zhang J. The effect of filler size on the properties of TPU/BN flexible thermal conductive composites prepared by fused filament fabrication. Polymer. 2024;296:126810.
17. Sut A, Metzsch-Zilligen E, Großhauser M, Pfaendner R, Schartel B. Rapid mass calorimeter as a high-throughput screening method for the development of flame-retarded TPU. Polym Degrad Stab. 2018;156:43–58.
18. Bashpa P, Bijudas K. Enhanced dielectric and thermal properties of thermoplastic polyurethane/multi-walled carbon nanotube composites. Mater Today Proc. 2022;51:2254–9.
19. Krishnasamy S, Dilip AA, Rahul A, Roshan RR, Yashwanth VT, Pugalzenthi S. Examining tribological and mechanical properties of PLA/TPU blends for footwear applications. Mater Circ Econ. 2024;6:25.
20. Hidnert P, Krider HS. Thermal expansion of aluminum and some aluminum alloys. J Res Natl Bur Stand. 1952;48:209–20.
21. Zhao H, He D, Xu H, Wang Y, Wang W, Shan Z. Comprehensive characterization of 3D-printed TPU/carbon black composites: morphological, thermal, and mechanical properties. Mater Today Commun. 2024;41:111099.
22. Ristić I, Cakić S, Vukić N, Teofilović V, Tanasić J, Pilić B. The influence of soft segment structure on the properties of polyurethanes. Polymers. 2023;15:3755.
23. Ouyang Y, Bai L, Tian H, Li X, Yuan F. Recent progress of thermal conductive ploymer composites: Al2O3 fillers, properties and applications. Compos Part Appl Sci Manuf. 2022;152:106685.
24. Jing X, Mi HY, Salick MR, Peng XF, Turng LS. Preparation of thermoplastic polyurethane/graphene oxide composite scaffolds by thermally induced phase separation. Polym Compos. 2014;35:1408–17. https://doi.org/10.1002/pc.22793.
25. Manap A, Mahalingam S, Vaithylingam R, Abdullah H. Mechanical, thermal and morphological properties of thermoplastic polyurethane composite reinforced by multi-walled carbon nanotube and titanium dioxide hybrid fillers. Polym Bull. 2021;78:5815–32.
26. Barick AK, Tripathy DK. Thermal and dynamic mechanical characterization of thermoplastic polyurethane/organoclay nanocomposites prepared by melt compounding. Mater Sci Eng A. 2010;527:812–23. https://doi.org/10.1016/j.msea.2009.10.063.
27. Ji Z, Liu W, Ouyang C, Li Y. High thermal conductivity thermoplastic polyurethane/boron nitride/liquid metal composites: the role of the liquid bridge at the filler/filler interface. Mater Adv. 2021;2:5977–85.
28. Su K-H, Su C-Y, Shih W-L, Lee F-T. Improvement of the thermal conductivity and mechanical properties of 3D-printed polyurethane composites by incorporating hydroxylated Boron nitride functional fillers. Materials. 2022;16:356.
29. Bahadur A, Shoaib M, Saeed A, Iqbal S. FT-IR spectroscopic and thermal study of waterborne polyurethane-acrylate leather coatings using tartaric acid as an ionomer. E-Polymers. 2016;16:463–74.
30. Behniafar H, Azadeh S. Transparent and flexible films of thermoplastic polyurethanes incorporated by Nano-SiO2 modified with 4, 4′-methylene Diphenyl diisocyanate. Int J Polym Mater Polym Biomater. 2015;64:1–6.
31. Tey WS, Cai C, Zhou K. A comprehensive investigation on 3D printing of polyamide 11 and thermoplastic polyurethane via multi jet fusion. Polymers (Basel). 2021;13:2139.
32. Banoriya D, Purohit R, Dwivedi RK. Wear performance of titanium reinforced biocompatible TPU. Adv Mater Process Technol. 2020;6:284–91.
33. Sattar R, Kausar A, Siddiq M. Advances in thermoplastic polyurethane composites reinforced with carbon nanotubes and carbon nanofibers: a review. J Plast Film Sheeting. 2015;31:186–224.

Publisher's note